HAL
open science

Simulation of two phase flow using a level set method: Application to bubbles and vesicle dynamics

Vincent Doyeux, Yann Guyot, Vincent Chabannes, Christophe Prud'Homme, Mourad Ismail

To cite this version:

Vincent Doyeux, Yann Guyot, Vincent Chabannes, Christophe Prud'Homme, Mourad Ismail. Simulation of two phase flow using a level set method: Application to bubbles and vesicle dynamics. ACOMEN 11 - 5th International Conference on Advanced COmputational Methods in ENgineering, Nov 2011, Liège, Belgium. pp.1-10. hal-00657152

HAL Id: hal-00657152

https://hal.science/hal-00657152

Submitted on 6 Jan 2012

HAL is a multi-disciplinary open access archive for the deposit and dissemination of scientific research documents, whether they are published or not. The documents may come from teaching and research institutions in France or abroad, or from public or private research centers.

L'archive ouverte pluridisciplinaire **HAL**, est destinée au dépôt et à la diffusion de documents scientifiques de niveau recherche, publiés ou non, émanant des établissements d'enseignement et de recherche français ou étrangers, des laboratoires publics ou privés.

Fifth International Conference on Advanced COmputational Methods in ENgineering (ACOMEN 2011)
Liège, Belgium, 14-17 November 2011
(c)University of Liège, 2011

Simulation of two phase flow using a level set method Application to bubbles and vesicle dynamics

V. Doyeux[1], Y. Guyot[1], V. Chabannes[1,2], C.Prud'homme[2] and M. Ismail[1]

[1] Université Grenoble 1 / CNRS, Laboratoire Interdisciplinaire de Physique / UMR 5588.
Grenoble, F-38041, France

[2] Université Grenoble 1 / CNRS, Laboratoire Jean Kuntzman / UMR 5224.
Grenoble, F-38041, France

e-mails: *vincent.doyeux@ujf-grenoble.fr*, {*christophe.prudhomme, mourad.ismail*}*@ujf-grenoble.fr*

Abstract

Level set method seems to be one of the most suitable solution for simulation of two phase flow systems. It can be implemented with different numerical methods (the commonly used one is Finite Differences Method **FDM**). In this work we chose to use a Finite Elements Method (**FEM**) to have more flexibility since it opens the way to high order discretization, irregular meshes and even high order geometry to handle large deformations.

A model of vesicle using a level set method has already been developed in [1] where the membrane of the vesicle is described only by adding a forcing term to the fluid equations. This model has the advantage to be coupled easily with any fluid solver accepting a forcing term as input.

In this paper, we present a new implementation of this model using a finite element approach. Firstly we show a validation of our two phase flow model on a well-known two phase flow system : the rising of a bubble. Then we show that we are able to recover the known equilibrium shapes of vesicles in a fluid at rest.

1 Introduction

Vesicles are systems of two fluids separated by a bi-layer membrane of phospholipids which has the property to be inextensible. These objects are biomimetics in the sense that they reproduce some biological objects behaviors. Specifically, vesicles have a mechanical behavior close to the one of Red Blood Cells (**RBC**) in a fluid flow. Indeed, it has been accepted for many years as a good model for RBC and they have been studied experimentally, theoretically and numerically. Simulating vesicles is very challenging in the sense that it combines fluid structure interaction and two phase flow systems. Several methods have already been developed such as lattice Boltzmann methods [2], boundary integral methods [3], or level set methods using **FDM** [1]. We propose in this paper a framework to simulate vesicles using finite element approximations. In the first part of the paper, we present a validation of the two phase flow solver. In the second part, we describe our model of vesicle and its validation using the equilibrium shapes of vesicles in a fluid at rest.

2 Level set description

2.1 Description

Let's define a bounded domain $\Omega \subset \mathbb{R}^p$ ($p = 2, 3$) decomposed into two subdomains Ω_1 and Ω_2. We denote Γ the interface between the two partitions. The goal of the level set method is to track implicitly the interface $\Gamma(t)$ moving at a velocity $\boldsymbol{u}$. The level set method has been described in [4] and its main ingredient is a continuous scalar function ϕ (the *level set* function) defined on the whole domain. This

function is chosen to be positive in Ω_1, negative in Ω_2 and zero on Γ. The motion of the interface is then described by the advection of the level set function :

$$\frac{\partial \phi}{\partial t} + \boldsymbol{u} \cdot \nabla \phi = 0. \tag{1}$$

A convenient choice for ϕ is a signed distance function to the interface. This function is given by equation (2) and we remark that $|\nabla \phi| = 1$ eases the numerical solution of equation (1), it reads

$$\phi(\boldsymbol{x}) = \begin{cases} \mathit{dist}(\boldsymbol{x}, \Gamma) & \boldsymbol{x} \in \Omega_1, \\ 0 & \boldsymbol{x} \in \Gamma, \\ -\mathit{dist}(\boldsymbol{x}, \Gamma) & \boldsymbol{x} \in \Omega_2, \end{cases} \tag{2}$$

where *dist* is the distance function : $\mathit{dist}(\boldsymbol{x}, \Gamma) = \min_{\boldsymbol{y} \in \Gamma} |\boldsymbol{x} - \boldsymbol{y}|$.

It's known that the advection equation (1) does not conserve the property $|\nabla \phi| = 1$. When $|\nabla \phi|$ is far from 1 we use a fast marching method (**FMM**) which resets ϕ as a distance function without moving the interface (see [5] for details about the fast marching method).

2.2 Interface related quantities

In two phase flow simulations, we need to define some quantities related to the interface such as the density, the viscosity, or interface forces. To this end, we introduce the smoothed Heaviside and delta functions :

$$H_\epsilon(\phi) = \begin{cases} 0, & \phi \leq -\epsilon, \\ \frac{1}{2}\left(1 + \frac{\phi}{\epsilon} + \frac{\sin(\frac{\pi\phi}{\epsilon})}{\pi}\right), & -\epsilon \leq \phi \leq \epsilon, \\ 1, & \phi \geq \epsilon. \end{cases}$$

$$\delta_\epsilon(\phi) = \begin{cases} 0, & \phi \leq -\epsilon, \\ \frac{1}{2\epsilon}\left(1 + \cos(\frac{\pi\phi}{\epsilon})\right), & -\epsilon \leq \phi \leq \epsilon, \\ 0, & \phi \geq \epsilon. \end{cases}$$

where ϵ is a parameter defining a numerical thickness of the interface. A typical value of ϵ is $1.5h$ (h being the mesh size).

We now easily define the density or the viscosity in the two domains using the Heaviside function. It reads: $\rho = \rho_2 + (\rho_1 - \rho_2) H_\epsilon(\phi)$ and similarly for the viscosity. The delta function is used to define quantities on the interface and we replace integrals over the interface by integrals over the entire domain using the smoothed delta function. If ϕ is a signed distance function, we have that :

$$\int_\Gamma 1 = \int_\Omega \delta \simeq \int_\Omega \delta_\epsilon(\phi). \tag{3}$$

If ϕ is not close enough to a distance function, then $\int_\Gamma 1 \simeq \int_\Omega |\nabla \phi| \delta_\epsilon(\phi)$ which still tends to the delta function as ϵ vanishes. However, if ϕ is not a distance function, the support of δ_ϵ can have a different size on each side of the interface. More precisely, the support of δ_ϵ is narrowed on the side where $|\nabla \phi| > 1$ and enlarged on regions where $|\nabla \phi| < 1$. It has been shown in [6] that replacing ϕ by $\psi = \frac{\phi}{|\nabla \phi|}$ has the property that $|\nabla \psi| \simeq 1$ near the interface and has the same iso-value 0 as ϕ. Thus, replacing ϕ by ψ in the delta function do not move the interface. Moreover the spread interface has the same size on each part of the level-set $\phi = 0$. It reads

$$\int_\Gamma 1 \simeq \int_\Omega \delta_\epsilon(\psi) = \int_\Omega \delta_\epsilon(\frac{\phi}{|\nabla \phi|}).$$

2.3 Numerical implementation and coupling with the fluid solver

We use the finite element C++ library `Feel++` [7, 8] to discretize and solve the problem. Equation (1) is solved using a stabilized finite element method. We have several stabilization methods at our disposal such as StreamLine Upwind Diffusion (SUPG), Galerkin Least Square (GLS) and Subgrid Scale (SGS). A general review of these methods is available in [9]. Other available methods include the Continuous Interior Penalty method (CIP) described in [10]. As to the Navier-Stokes solver, it is described in [11]. The coupling algorithm is presented in Algorithm 1

Algorithm 1 Level set - Navier Stokes Coupling

while time $<$ final time **do**
  Calculate $\rho(\phi^{n-1})$, $\mu(\phi^{n-1})$, and $F(\phi^{n-1})$
  Solve Navier Stokes equation to get $\boldsymbol{u^n}$
  Advect level set function with $\boldsymbol{u^n}$ to obtain ϕ^n
end while

3 Validation of two phase flow solver

We now turn to the validation of our framework using the benchmark [12].

3.1 Benchmark problem

The benchmark objective is to simulate the rise of a 2D bubble in a newtonian fluid. The equations solved are the incompressible Navier Stokes equations for the fluid and the advection for the level set:

$$\rho(\phi(\boldsymbol{x}))\left(\frac{\partial \boldsymbol{u}}{\partial t}+\boldsymbol{u}\cdot\nabla\boldsymbol{u}\right)+\nabla p-\nabla\cdot\left(\mu(\phi(\boldsymbol{x}))(\nabla\boldsymbol{u}+(\nabla\boldsymbol{u})^T)\right) = \rho(\phi(\boldsymbol{x}))\boldsymbol{g}, \tag{4}$$

$$\nabla\cdot\boldsymbol{u} = 0, \tag{5}$$

$$\frac{\partial\phi}{\partial t}+\boldsymbol{u}\cdot\nabla\phi = 0, \tag{6}$$

where ρ is the density of the fluid, μ its viscosity, and $\boldsymbol{g}\approx(0,0.98)^T$ is the gravity acceleration.

The computational domain is $\Omega\times]0,T]$ where $\Omega=(0,1)\times(0,2)$ and $T=3$. We denote Ω_1 the domain outside the bubble $\Omega_1=\{\boldsymbol{x}|\phi(\boldsymbol{x})>0\}$, Ω_2 the domain inside the bubble $\Omega_2=\{\boldsymbol{x}|\phi(\boldsymbol{x})<0\}$ and Γ the interface $\Gamma=\{\boldsymbol{x}|\phi(\boldsymbol{x})=0\}$. On the lateral walls, slip boundary conditions are imposed, *i.e.* $\boldsymbol{u}\cdot\boldsymbol{n}=0$ and $\boldsymbol{t}\cdot(\nabla\boldsymbol{u}+(\nabla\boldsymbol{u})^T)\cdot\boldsymbol{n}=0$ where $\boldsymbol{n}$ is the unit normal to the interface and $\boldsymbol{t}$ the unit tangent. No slip boundary conditions are imposed on the horizontal walls *i.e.* $\boldsymbol{u}=\boldsymbol{0}$. The initial bubble is circular with a radius $r_0=0.25$ and centered on the point $(0.5,0.5)$. A surface tension force $\boldsymbol{f}_{st}$ is applied on Γ, it reads using equation (3):

$$\boldsymbol{f}_{st}=\int_\Gamma\sigma\kappa\boldsymbol{n}\simeq\int_\Omega\sigma\kappa\boldsymbol{n}\delta_\epsilon(\phi), \tag{7}$$

where σ stands for the surface tension between the two fluids, $\boldsymbol{n}$ the unit vector normal to the interface defined as $\boldsymbol{n}=\frac{\nabla\phi}{|\nabla\phi|}$ and $\kappa=\nabla\cdot(\frac{\nabla\boldsymbol{\phi}}{|\nabla\phi|})$ is the curvature of the interface.

We denote with indices 1 and 2 the quantities relative to the fluid in domain respectively Ω_1 and Ω_2. The parameters of the benchmark are ρ_1, ρ_2, μ_1, μ_2 and σ. We define two dimensionless numbers: firstly, the Reynolds number which is the ratio between inertial and viscous terms and is defined as : $Re=\dfrac{\rho_1\sqrt{|\boldsymbol{g}|(2r_0)^3}}{\mu_1}$; secondly, the Eötvös number represents the ratio between the gravity force and the surface tension $E_0=\dfrac{4\rho_1|\boldsymbol{g}|r_0^2}{\sigma}$. The table 1 reports the values of the parameters used for two different test cases proposed in [12].

Tests	ρ_1	ρ_2	μ_1	μ_2	σ	Re	E_0
Test 1 (ellipsoidal bubble)	1000	100	10	1	24.5	35	10
Test 2 (skirted bubble)	1000	1	10	0.1	1.96	35	125

Table 1: Numerical parameters taken for the benchmarks.

The quantities measured in [12] are $\boldsymbol{X_c}$ the center of mass of the bubble, $\boldsymbol{U_c}$ its velocity and the circularity defined as the ratio between the perimeter of a circle which has the same area and the perimeter of the bubble which reads $c = \dfrac{2(\pi \int_{\Omega_2} 1)^{\frac{1}{2}}}{\int_\Gamma 1}$.

3.2 Results

In the first test case, the bubble reaches a stationary circularity and its topology does not change. The velocity increases until it attains a maximum then decreases to a constant value. Figure 1 shows the results obtained with different mesh sizes. Table 2 shows a comparison of our results with those of [12]. We monitor c_{min} the minimum of the circularity, $t_{c_{min}}$ the time to attain this minimum, $u_{c_{max}}$ the maximum velocity, $t_{u_{c_{max}}}$ the time to reach it, and $y_c(t = 3)$ the position of the bubble at final time ($t = 3$).

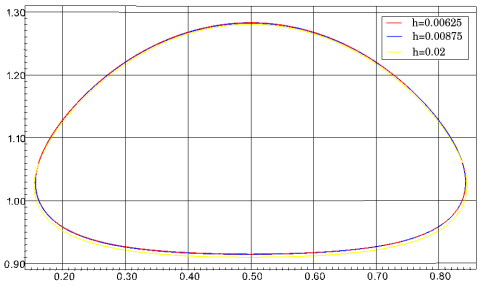

(a) Shape of ellipsoidal bubble at final time ($t = 3$).

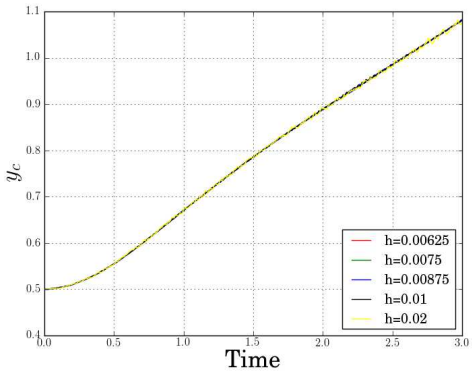

(b) y_c vertical position of the ellipsoidal bubble.

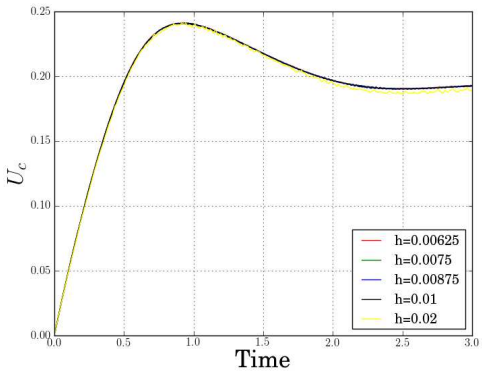

(c) Vertical velocity of the ellipsoidal bubble.

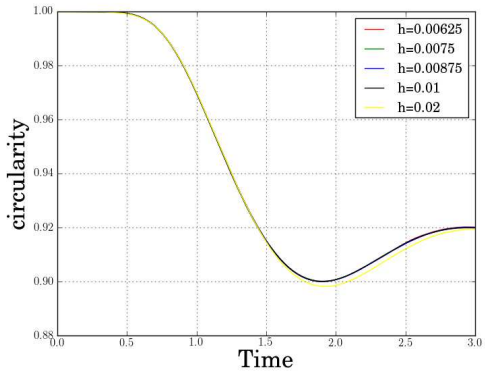

(d) Circularity of the ellipsoidal bubble.

Figure 1: Results for the ellipsoidal bubble

In the second test case, the bubble gets more deformed because of the lower surface tension. Some filaments (skirts) appear at the bottom. The velocity attains two local maxima. Figure 2 displays these

	c_{min}	$t_{c_{min}}$	$u_{c_{max}}$	$t_{u_{c_{max}}}$	$y_c(t=3)$
lower bound	0.9011	1.8750	0.2417	0.9213	1.0799
upper bound	0.9013	1.9041	0.2421	0.9313	1.0817
h=0.00625	0.9001	1.9	0.2412	0.9248	1.0815
h=0.0075	0.9001	1.9	0.2412	0.9251	1.0812
h=0.00875	0.89998	1.9	0.2410	0.9259	1.0814
h=0.01	0.8999	1.9	0.2410	0.9252	1.0812
h=0.02	0.8981	1.925	0.2400	0.9280	1.0787

Table 2: Results comparison between benchmarks values (lower and upper bounds) and ours for ellipsoidal bubble.

results. Table 3 shows the comparison with the benchmark results. We monitor the same quantities as in the previous test case except that we add the second maximum velocity $u_{c_{max_2}}$, and the time to reach it $t_{u_{c_{max_2}}}$.

(a) Shape of squirted bubble at final time ($t = 3$).

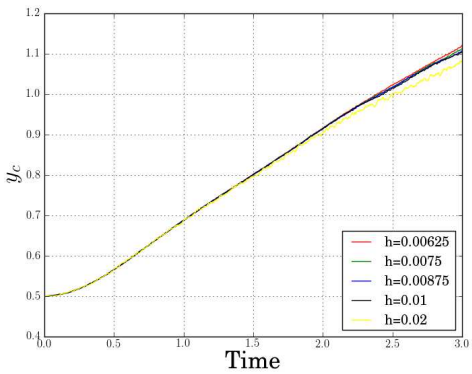

(b) y_c vertical position of the skirted bubble.

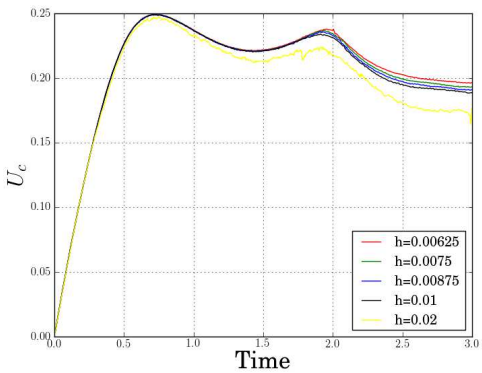

(c) Vertical velocity of the skirted bubble.

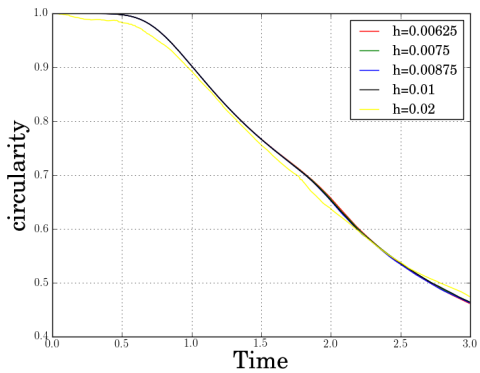

(d) Circularity of the skirted bubble.

Figure 2: Results for the skirted bubble.

	c_{min}	$t_{c_{min}}$	$u_{c_{max_1}}$	$t_{u_{c_{max_1}}}$	$u_{c_{max_2}}$	$t_{u_{c_{max_2}}}$	$y_c(t=3)$
lower bound	0.4647	2.4004	0.2502	0.7281	0.2393	1.9844	1.1249
upper bound	0.5869	3.0000	0.2524	0.7332	0.2440	2.0705	1.1380
h=0.00625	0.4616	2.995	0.2496	0.7574	0.2341	1.8828	1.1186
h=0.0075	0.4646	2.995	0.2495	0.7574	0.2333	1.8739	1.1111
h=0.00875	0.4629	2.995	0.2494	0.7565	0.2324	1.8622	1.1047
h=0.01	0.4642	2.995	0.2493	0.7559	0.2315	1.8522	1.1012
h=0.02	0.4744	2.995	0.2464	0.7529	0.2207	1.8319	1.0810

Table 3: Results comparison between benchmarks values (lower and upper bounds) and ours for skirted bubble

4 Vesicle dynamics simulation

4.1 Model

The model usually admitted for vesicle membrane assumes three properties : *(i)* the membrane has a bending energy E_b, called the Canham, Helfrich energy [13, 14], *(ii)* the inner fluid is incompressible, so the total surface of the vesicle is conserved and finally *(iii)* the membrane is quasi inexentensible, so the local perimeter is conserved over the time.

4.1.1 The bending energy

The bending energy can be written in 2D as follows:

$$E_b = \int_\Gamma \frac{k_B}{2}\kappa^2 \tag{8}$$

where k_B is the bending modulus (a typical value for phospholipidic membrane is $k_B \approx 10^{-19}$ J). A derivation of this energy gives a bending force, its expression is given in [15] and reads :

$$\boldsymbol{F_b^*} = \int_\Gamma \frac{k_B}{2}\left[\frac{\kappa^3}{2} + \boldsymbol{t}\cdot\nabla(\boldsymbol{t}\cdot\nabla\kappa)\right]\boldsymbol{n}, \tag{9}$$

(note that equation (9) has the opposite sign that the one in [15] because our definition of the curvature has an opposite sign). A more general equation has been proposed in [1] using the virtual power method : $\frac{dE_b}{dt} = -\int_\Omega \boldsymbol{F_b}\cdot\boldsymbol{u}$. The derivation of the force and the link between this expression and the equation (9) are detailed in [1], one obtains in 2D :

$$\boldsymbol{F_b} = \int_\Omega k_B\nabla\cdot\left[\frac{-\kappa^2}{2}\boldsymbol{n} + \frac{1}{|\nabla\phi|}\left(\boldsymbol{t}\cdot\nabla\{|\nabla\phi|\kappa\}\right)\boldsymbol{t}\right]\delta_\epsilon\boldsymbol{n}. \tag{10}$$

4.1.2 Membrane inextensibility

In many models, the local area of the vesicle is conserved by adding a Lagrange multiplier which ensures the membrane inextensibility as in [15, 16, 17]. In [6], the authors show the possibility to get the quasi inextensibility of the membrane by adding an elastic force using the derivative of an elastic energy. They show that the stretching of the interface is recorded in the gradient modulus of ϕ. Indeed, under the assumption that the flow is incompressible, one can write a constitutive law of the stretching related to $|\nabla\phi|$. The elastic energy reads :

$$E_{el} = \int_\Omega E(|\nabla\phi|)\delta_\epsilon,$$

with $E(|\nabla\phi|)$ a constitutive law of the membrane such that $E(1) = 0$ (no initial stretching). A simple definition of $E'(\nabla\phi)$ (the derivative of E) can be used as a linear law : $E'(|\nabla\phi|) = \Lambda(|\nabla\phi| - 1)$. In our case, we take $E'(|\nabla\phi|) = \Lambda \max((|\nabla\phi| - 1), 0)$ which ensures that there is no force when the stretching is not positive. By differentiating the energy, it has been shown in [6] that one can write the elastic force as :

$$\boldsymbol{F_{el}} = \int_\Omega \{\nabla E'(|\nabla\phi|) - \nabla \cdot [E'(|\nabla\phi|)\boldsymbol{n}]\, \boldsymbol{n}\}\, \delta_\epsilon. \tag{11}$$

One can see that choosing to add a force to maintain incompressibility has some advantages. For example, we can add complexity to the model such as changing the constitutive law of E' (*e.g.* a more rigid part which could take into account the cytoskeleton of a red blood cell) or add a new force like a surface tension force.

The main drawback is that in general, this technique leads to a larger variation of the surface area than the ones using Lagrange multipliers. Note also that in this model, we need to keep the information of $\nabla\phi$ so that to avoid reinitialization which resets $|\nabla\phi| = 1$ and *forgets* the stretching information. The conservation of the total surface of the vesicle is better than the conservation of the local perimeter since it is enforced by the incompressibility of the fluid. Finally, we just have to add forcing terms $\boldsymbol{F_b}$ and $\boldsymbol{F_{el}}$ to equation (4) to simulate the presence of the membrane.

4.2 Dimensionless equations

To scale the different parameters of the simulation we use dimensionless numbers. One can easily write the Navier-Stokes equations with forcing terms $\boldsymbol{F_b}$ and $\boldsymbol{F_{el}}$ using dimensionless numbers as (see [1] for details) :

$$\begin{aligned} & Re\, \rho^*\left(\frac{\partial \boldsymbol{u^*}}{\partial t^*} + \boldsymbol{u^*} \cdot \nabla^* \boldsymbol{u^*}\right) - \nabla^* \cdot (\eta^* D(\boldsymbol{u^*})) + \nabla^* p^* \\ = \quad & \left\{ \frac{1}{W_e}\left[\nabla^* E'^* - \nabla^* \cdot [E'^* \boldsymbol{n}]\boldsymbol{n}\right] + \frac{1}{C_k}\nabla^* \cdot \left[\frac{-\kappa^{*2}}{2}\boldsymbol{n} + \frac{1}{|\nabla^*\phi^*|}\left(\boldsymbol{t} \cdot \nabla^*\{|\nabla^*\phi^*|\kappa^*\}\right)\boldsymbol{t}\right]\right\} \delta_\epsilon, \end{aligned}$$

where the quantities denoted with a star are dimensionless quantities using references parameters : $x = Lx^*$, $u = Uu^*$, $\eta = \eta_{ref}\eta^*$ and $\rho = \rho_{ref}\rho^*$. The Reynolds number is given by $Re = \dfrac{\rho_{ref} L U}{\eta_{ref}}$. The two other dimensionless numbers are $C_k = \dfrac{\eta_{ref} U L^2}{k}$ the capillary number, and the Weissenberg number $W_e = \dfrac{\eta_{ref} U}{\Lambda}$.

4.3 Equilibrium shape

The first known behavior on which we can validate our code is the shape that takes a vesicle in a fluid at rest. Indeed, the vesicle takes the shape which minimizes its Helfrich energy (8). Since there is no characteristic velocity imposed, we take a dimensionless number which takes into account the ratio between the curvature force and the elastic force $R_f = \dfrac{C_k}{W_e} = \dfrac{L^2\Lambda}{k}$ where we take as reference length L the radius of a circle having the same perimeter than the vesicle. We then fix this parameter to $5 \cdot 10^4$. The other parameter is the reduced volume α, which measures how much the vesicle is deflated. It is defined as the ratio between the area of the vesicle and the area of a disk having the same perimeter than the vesicle : $\alpha = \dfrac{4\pi A}{P^2}$. Vesicles are initialized as ellipses having the same perimeter, only their surface changes to decrease α. The vesicle being out of equilibrium starts to move and induce a fluid flow around it. Figure 3 shows our results for different reduced volume. Obviously for $\alpha = 1$ the equilibrium shape of the vesicle is a sphere (circle in 2D). It is interesting to see that for a reduced volume lower than 0.5, the vesicle takes a biconcave shape which is also typical for red blood cells. The loss of perimeter is of the order of few percents which is higher than the one obtained using a Lagrange multiplier method

to enforce perimeter conservation. The loss of surface is lower that one percent since it is enforced by the divergence-free velocity of the fluid.

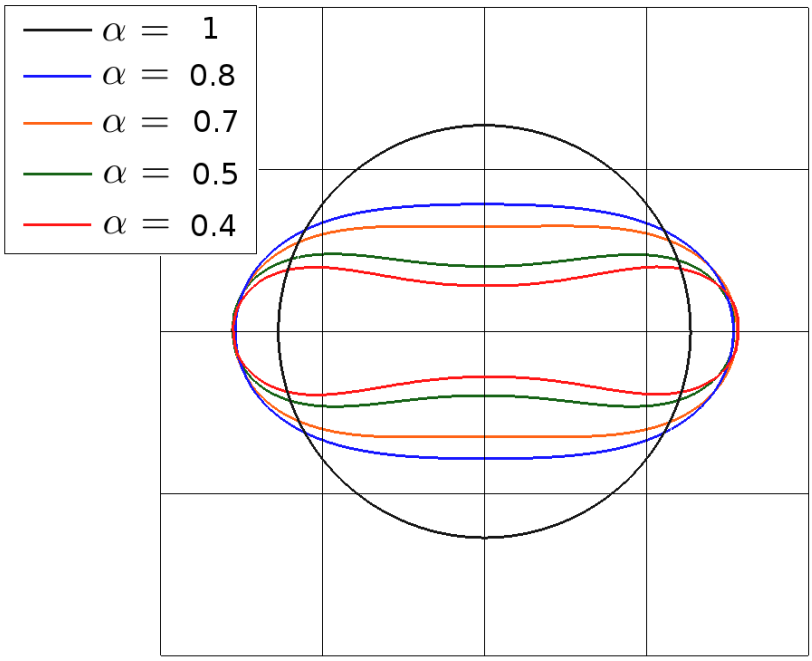

Figure 3: Equilibrium shapes of vesicles for different reduce volumes.

5 Conclusion

We have shown that we have validated our framework using finite element approximations of two phase flow simulations. We also presented the first results obtained on vesicle simulation which proves that we are able to capture the basic behavior of these objects. In a near future, further tests on basic behavior is expected such as the tumbling motion and the migration of a vesicle in a Poiseuille flow. Another interesting improvement will be to add many vesicles in the same simulation to mimic more realistic biological flows.

Acknowledgments

This work is financially supported by the Région Rhône-Alpes (ISLE/CHPID project) and the ANR (MOSICOB project).

References

[1] E. Maitre, C. Misbah, P. Peyla, and A. Raoult. Comparison between advected-field and level-set methods in the study of vesicle dynamics. *ArXiv e-prints*, May 2010.

[2] B. Kaoui, J. Harting, and C. Misbah. Two-dimensional vesicle dynamics under shear flow: Effect of confinement. *pre*, 83(6):066319–+, June 2011.

[3] J. Beaucourt, F. Rioual, T. Seacuteon, T. Biben, and C. Misbah. Steady to unsteady dynamics of a vesicle in a flow. *Phys. Rev. E*, 69(1):011906–, January 2004.

[4] Stanley Osher and James A. Sethian. Fronts propagating with curvature dependent speed: Algorithms based on hamilton-jacobi formulations. *Journal of Computational Physics*, 79(1):12–49, 1988.

[5] Christophe Winkelmann. *Interior penalty finite element approximation of Navier-Stokes equations and application to free surface flows*. PhD thesis, 2007.

[6] Emmanuel Maitre Georges-Henri Cottet. A level set method for fluid-structure interactions with immersed surfaces. *Mathematical Models and Methods in Applied Sciences*.

[7] C. Prud'homme, V. Chabannes, and G. Pena. Feel++: Finite Element Embedded Language in C++. Free Software available at http://www.feelpp.org. Contributions from A. Samake, V. Doyeux, M. Ismail and S. Veys.

[8] Christophe Prud'homme. A domain specific embedded language in C++ for automatic differentiation, projection, integration and variational formulations. *Scientific Programming*, 14, 2006.

[9] R.P. Bonet Chaple. Numerical stabilization of convection-diffusion-reaction problems. Technical report, 2006.

[10] Erik Burman and Peter Hansbo. Edge stabilization for the generalized stokes problem: A continuous interior penalty method. *Computer Methods in Applied Mechanics and Engineering*, 195(19-22):2393–2410, April 2006.

[11] V. Chabannes, G. Pena, and C.Prud'homme. High order fluid structure interaction in 2d and 3d. application to blood flow in arteries. In *Fifth International Conference on Advanced COmputational Methods in ENgineering (ACOMEN 2011)*, 2011.

[12] S. Hysing, S. Turek, D. Kuzmin, N. Parolini, E. Burman, S. Ganesan, and L. Tobiska. Quantitative benchmark computations of two-dimensional bubble dynamics. *International Journal for Numerical Methods in Fluids*, 60(11):1259–1288, 2009.

[13] P.B. Canham. The minimum energy of bending as a possible explanation of the biconcave shape of the human red blood cell. *Journal of Theoretical Biology*, 26(1):61 – 81, 1970.

[14] W Helfrich. Elastic properties of lipid bilayers: theory and possible experiments. *Z Naturforsch C*, 28(11):693–703–, 1973.

[15] T. Biben and C. Misbah. Tumbling of vesicles under shear flow within an advected-field approach. *Phys Rev E*, 67(3):031908–+, March 2003.

[16] Badr Kaoui, Alexander Farutin, and Chaouqi Misbah. Vesicles under simple shear flow: Elucidating the role of relevant control parameters. *Phys. Rev. E*, 80(6):061905, Dec 2009.

[17] A. Laadhari, C. Misbah, and P. Saramito. On the equilibrium equation for a generalized biological membrane energy by using a shape optimization approach. *Physica D: Nonlinear Phenomena*, 239(16):1567 – 1572, 2010.